Band gap of amorphous and well-ordered Al_2O_3 on $Ni_3Al(100)$

I. Costina[a] and R. Franchy
Institut für Schichten und Grenzflächen (ISG3) des Forschungszentrum Jülich, D-52425 Jülich, Germany

(Received 26 February 2001; accepted for publication 27 April 2001)

The vibrational and electronic properties of amorphous and well-ordered alumina formed on $Ni_3Al(100)$ were investigated using high-resolution electron energy loss spectroscopy. The structure of well-ordered alumina was analyzed by low-energy electron diffraction. The amorphous Al_2O_3 films are prepared by adsorption of O_2 at room temperature, while the well-ordered Al_2O_3 are obtained by direct oxidation of Ni_3Al at 1150 K. The band gap energy is ~3.2 and ~4.3 eV for amorphous alumina and well-ordered alumina thin films respectively. The lowering of the band gap with respect to the bulk value of Al_2O_3 is associated with defect-induced states located in the band gap. © *2001 American Institute of Physics.* [DOI: 10.1063/1.1380403]

Alumina (Al_2O_3) presents a great interest in various application areas such as catalysis, coatings, microelectronics, and thin-film devices.[1] The latter applications take into account the electronic properties of Al_2O_3. Among the electronic properties, the band gap has been a subject of discussion particularly in the case of thin Al_2O_3 films.[2,3] The decrease of the energy band gap value reported for thin α-alumina[4,5] and γ-alumina[2] is explained in terms of the appearance of a metallic characteristic in the alumina surface layers[4] or due to some defect levels located in the band gap.[2] Such defect states were found also in Al_2O_3 film grown on Al(111) and they were related to intermediate Al oxidation states.[6] The tunneling experiments performed on Al_2O_3 film[7] showed an asymmetric potential barrier. This has been interpreted in the terms of the existence of a semiconductor-like phase at the metal–insulator interface.

In this letter we report the investigations of the growth of Al_2O_3 on $Ni_3Al(100)$, focusing our attention on the band gap of the thin oxide films. We observed a decrease in the band gap of Al_2O_3 thin films with respect to the bulk value suggesting the appearance of defect levels located in the band gap. Ni–Al compounds, in various stoichiometry, are well known as suitable alloys for the preparation of thin alumina films through direct oxidation.[8] In general, the formation of Al_2O_3-oxide is thermodynamically favored, having a heat of formation ($\Delta H_f = -1675.7 \pm 1.3\,\mathrm{kJ\,mol^{-1}}$) higher than the corresponding value for NiO ($\Delta H_f = -240\,\mathrm{kJ\,mol^{-1}}$).[9] Ni_3Al crystallizes in the LI_2 (Cu_3Au-type) structure which is cubic (space group $Pm3m$) and contains four atoms per unit cell.[10] This is a fcc structure with Al atoms located at the cube corners and Ni atoms occupying the face centers. There are two possible terminations for the top atomic layer in the case of $Ni_3Al(100)$ surface, the first one contains 50% Ni–50% Al composition (mixed layer), and the second possible configuration being 100% Ni. The first principles calculation of cohesive energy and low-energy electron diffraction (LEED) investigations[10] suggest that the mixed-layer surface is more stable, but when the oxide is present, a ''termination inversion'' occurs stabilizing the 100% Ni structure as topmost layer.

The experiments were performed in a UHV system[11] with facilities for Auger electron spectroscopies, LEED, and high-resolution electron energy loss spectroscopy (HREELS). The $Ni_3Al(100)$ single crystal was cut by spark erosion and polished mechanically. It was oriented using an x-ray diffractometer with an accuracy of 0.1°. The clean $Ni_3Al(100)$ surface was obtained after several cycles of argon ions sputtering (1 keV; 5.4 μA/cm^2) followed by annealing at 1400 K. The HREEL spectrometer is based on optimized 127° cylindrical deflectors,[12] with a typical resolution of 2–3 meV, and has been operated in two modes. The first mode is used to study the vibrational properties of aluminum oxide film. In order to observe the electronic transitions the spectrometer was operated in a second mode where the loss spectra cover a energy range up to 10 eV.

The adsorption of 500 L O_2 (saturation) at 300 K led to a diffuse LEED pattern which is not shown here. After annealing at 1150 K, the LEED pattern showed very sharp spots and very low background, indicating the formation of a well-ordered oxide. A similar LEED pattern is also obtained when $Ni_3Al(100)$ surface is directly oxidized at 1150 K. A representative LEED pattern obtained by the oxidation of $Ni_3Al(100)$ surface with 2000 L O_2 at 1150 K is given in Fig. 1. The oxidation has been performed at a pressure of 3×10^{-6} mbar. A similar hexagonal structure of aluminum oxide in LEED pattern was reported in Ref. 13. The lattice constant estimated from LEED was found to correspond to O^{2-} periodicity. The coincidence of unit vector lengths estimated from LEED with the length of the basis vectors along the (111) plane of γ'-Al_2O_3 suggested that this is the phase formed on Ni_3Al and that the oxide growing with the (111) plane parallel to the substrate surface plane.[13]

Figure 2 shows typical HREEL spectra of the $Ni_3Al(100)$ surface oxidized at room temperature and at 1150 K. The sample oxidized at 300 K shows two broad losses at 575 and 868 cm^{-1}. A similar HREEL spectrum was reported for amorphous Al_2O_3.[14] Therefore, we conclude that the oxidation at room temperature of $Ni_3Al(100)$ leads to the formation of an amorphous Al_2O_3, whereas the direct oxidation at 1150 leads to a HREEL spectrum with three losses located at 415, 640, and 875 cm^{-1}. The vibrational losses are similar to those obtained by Franchy *et al.*[15] for γ'-Al_2O_3 grown on

[a]Electronic mail: j.costina@fz-juelich.de

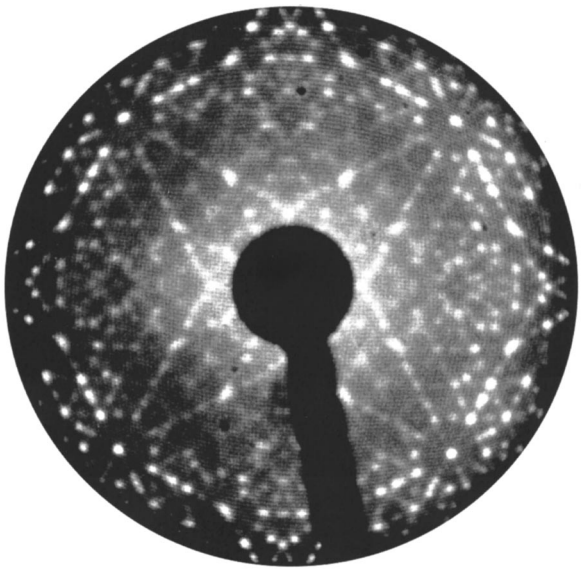

FIG. 1. LEED pattern of $Al_2O_3/Ni_3Al(100)$. The $Ni_3Al(100)$ surface was oxidized at 1150 K with 2000 L of O_2. $E_p=54$ eV.

NiAl(111) (losses at 427, 637, and 887 cm^{-1}). Becker *et al.*[16] found a very similar spectrum in the case of γ'-Al_2O_3 on $Ni_3Al(111)$ with losses at 440, 647, and 909 cm^{-1}. As the dielectric theory is the theoretical framework of the HREELS, the comparison between calculated and measured spectra can give some important indications about structure and thickness of the films.[17] We calculated the theoretical HREEL spectra for amorphous and well-ordered oxide using a program[18] which allows to simulate the HREEL spectrum for electrons specularly reflected at the surface. The parameters used for the simulation of the HREEL spectra for amorphous and well-ordered γ-Al_2O_3 are taken from Ref. 19. The Ni_3Al substrate is represented through a Drude term with $\omega_p=7.4$ eV and $\gamma_{Ni_3Al}=0.03$.[20] The calculated spectra are also represented in Fig. 2 (solid line). For the amorphous Al_2O_3 a slight disagreement can be observed between the calculated and the experimental spectra concerning the frequency positions and the intensity ratio of the losses. Amorphous Al_2O_3 has a short range order and can be described as clusters of randomly oriented oxygen fcc lattices, with Al cations sitting in tetrahedral interstices. The shift of measured loss peaks with respect to the calculated ones was interpreted as the existence of different Al–O–Al bond angles and lengths within the AlO_4 tetrahedra.[14] A similar effect was found for O/Si(111).[21] Another reasons could be the failure of the dielectric theory in producing the correct frequency position of the surface energy-loss peaks in the case of ultrathin films (less than ~2 nm).[22] A better agreement between calculated and experimental spectra was found in the case of well-ordered film. The best fit was obtained considering a thickness of 5 Å for the well-ordered Al-oxide. This value has to be considered only as approximate, taking into account the number of parameters used for calculation.

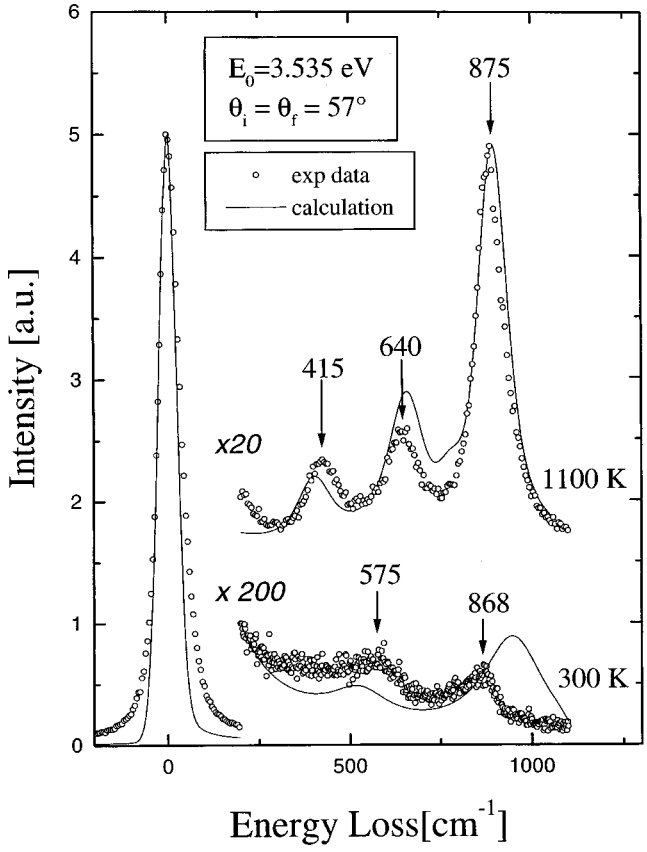

FIG. 2. HREEL spectra of $Ni_3Al(100)$ exposed to 500 L O_2 at 300 K (bottom) and 2000 L O_2 at 1150 K (top). The experimental data are represented by circles, and the calculated spectra by solid lines.

In order to measure electronic transitions, the HREEL spectrometer was set in the second operation mode. The spectra were recorded using a primary energy of 32 eV. In Figs. 3(a) and 3(b) the loss features up to 10 eV energy loss are given for amorphous and well-ordered alumina, respectively. The elastic beam, and the vibrational losses are not shown (i.e., losses below ~0.2 eV). The spectrum of the amorphous Al_2O_3 shows a shoulder at 0.7 eV and a broad loss feature at an onset of ~3.2 eV. In the case of the well-ordered Al-oxide, the broad feature starts at ~4.3 eV. The loss probability is proportional to the joint density of states, disregarding the matrix elements effects.[14] Using a very coarse approximation of parabola around the maximum (minimum) of the valence (conduction) band the loss probability is proportional to $\Theta(\hbar\omega-E_g)\sqrt{(\hbar\omega-E_g)}$ (with the Heaviside step function Θ). The fit of our data with this function yields $E_g\cong 3.2$ eV for amorphous oxide and $E_g \cong 4.3$ eV for the well-ordered oxide.

The band gap of the bulk γ-Al_2O_3 has a value of 8.7 eV.[23] In order to understand the decreasing of the band gap value, we have to make some remarks concerning the interband transitions. For a one-electron model, neglecting the relaxation effects in photoemission transition or excitonic efects in interband transition, the interband transition can be described as an electronic excitation from bound state (valence or core) to an unoccupied state located in the conduction band.[24] The onset of the broad energy losses in the HREEL spectrum can be associated with an interband transition. If the energy losses are lower than the energy gap, this can be interpreted as electronic transitions between the valence band and unoccupied states located in the band gap.[3] As we have mentioned before, the states could be induced by defects. This hypothesis is supported also by the density of states calculation of Ciraci and Batra[25] which obtained empty energy levels located in the band gap supposing the existence

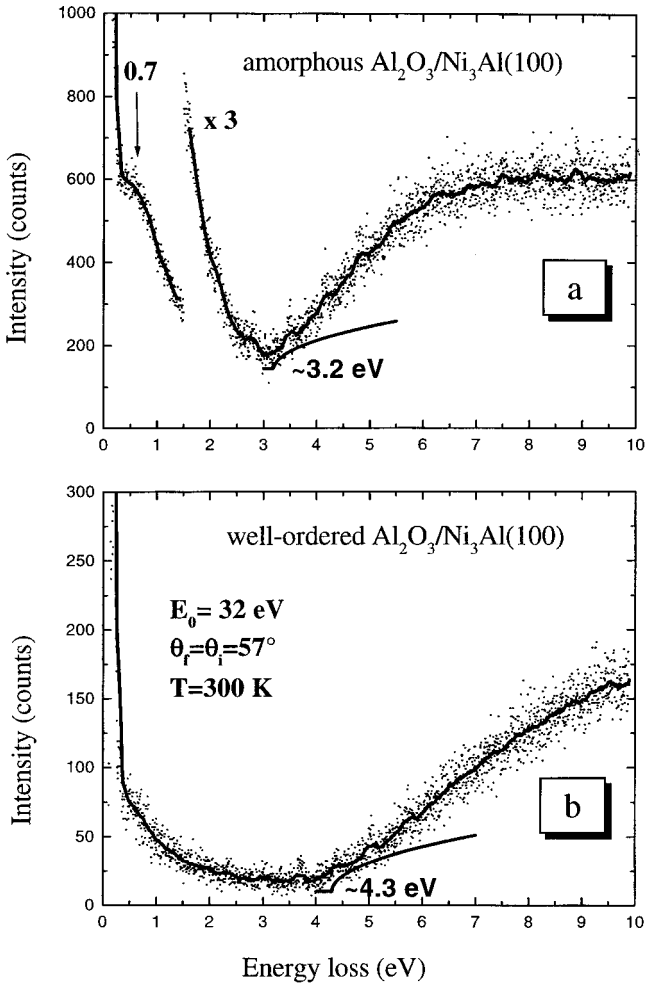

FIG. 3. Wide range HREEL spectra of (a) amorphous alumina and (b) well-ordered alumina formed on $Ni_3Al(100)$ surface. The primary electron energy was 32 eV.

of ideal vacancies in Al_2O_3. In Ref. 3 the authors show that the band gap for thin γ-Al_2O_3 film is dramatically reduced up to 2.6 eV. The appearance of the empty levels induced by defects located in the band gap is considered as a reason for the decrease of the band gap value. The dangling Al *spz* bond at the surface is also responsible for the existence of a discrete level located below the conduction band minimum energy. Taking into account this small value of band gap the authors do not consider the γ-Al_2O_3 thin film as isolator, but as a phase with different properties characterized by the decrease of the ionicity of the oxygen sites. In the case of the $(\sqrt{31}\times\sqrt{31})R\pm 9°$ reconstructed surface of α-$Al_2O_3(0001)$[4] the band gap is also found to be smaller than it's bulk value. In this case no empty levels are detected in the band gap. The decreasing of the band gap from 8.3 to 7 eV is interpreted in terms of rehybridization between O $2p$ and Al $3s-3p$ and, consequently, to the modification of charge transfer between aluminum and oxygen. In the case of Al_2O_3 the upper valence band is derived from O $2p$ states and the conduction band is derived from Al $3s$ and $3p$ states.[26] In the case of θ-Al_2O_3 formed on NiAl(001), Bartolucci *et al.*[27] have found a band gap value of about 7.4 eV which is also diminished with respect to the value for the bulk.

In our studies a broad loss feature in HREEL spectra starts at about 3.2 eV for the amorphous Al-oxide and at 4.3 eV for the well-ordered Al-oxide. In the case of an ideal, defect-free crystalline insulator, the intensity should increase abruptly at the energy gap. In contrast, in our experiments these sharp edges are not present. However, the energy levels induced by defects, which are located in the band gap, diminish the band gap energy. In amorphous semiconductors, it was also found that a distribution of tail states encroaches into the otherwise empty band gap region.[28] The analysis shows that tail states are localized by the site disorder and they are responsible for many of the unique properties exhibited by amorphous semiconductors.[29,30]

In conclusion, we have measured the band gap of ultrathin amorphous and well-ordered Al_2O_3 formed on $Ni_3Al(100)$. In both cases the values obtained are strongly diminished with respect to the bulk values. We associate the lowering of the band gap value of thin alumina film on Ni_3Al with the existence of defect induced states encroached in the band gap region.

This work was supported by the HGF project "Magnetoelectronics."

[1] N. S. Stoloff, C. T. Liu, and S. C. Deevi, Intermetallics **8**, 1313 (2000).
[2] A. Jimenéz-Gonzales and D. Schmeisser, Surf. Sci. **250**, 59 (1991).
[3] B. Ealet, M. H. Elyakhloufi, E. Gillet, and M. Ricci, Thin Solid Films **250**, 92 (1994).
[4] M. Gautier, J. P. Duraud, L. P. Van, and M. J. Guittet, Surf. Sci. **250**, 71 (1991).
[5] S. Andersson, P. A. Brühwiller, M. F. A. Sandell, J. Libuda, A. Giertz, B. Brena, A. J. Maxwell, M. Bäumer, H.-J. Freund, and N. Mårtensson, Surf. Sci. **442**, L964 (1999).
[6] A. Bianconi, R. Z. Bachrach, S. H. Hagstrom, and S. A. Flodström, Phys. Rev. B **19**, 2837 (1979).
[7] J. C. Fisher and I. Giaever, J. Appl. Phys. **32**, 172 (1961).
[8] R. Franchy, Surf. Sci. Rep. **38**, 195 (2001).
[9] *CRC Handbook of Chemistry and Physics*, edited by D. R. Lide (CRC Press, Boca Raton, FL, 1994).
[10] D. Sondericker, F. Jona, and P. M. Marcus, Phys. Rev. B **33**, 900 (1986).
[11] P. Gassmann, Ph.D. thesis, RTWH Aachen, 1996.
[12] H. Ibach, *Electron Energy Loss Spectrometers, The Technology of High Performance*, Springer Series in Optical Science, Vol. 63 (Springer, Heidelberg, 1991).
[13] U. Bardi, A. Atrei, and G. Rovida, Surf. Sci. **268**, 87 (1992).
[14] P. Gassmann, R. Franchy, and H. Ibach, Surf. Sci. **319**, 95 (1994).
[15] R. Franchy, J. Masuch, and P. Gassmann, Appl. Surf. Sci. **93**, 31 (1996).
[16] C. Becker, J. Kandler, H. Raaf, R. Linke, T. Pelster, M. Dräger, M. Tanemura, and K. Wandelt, J. Vac. Sci. Technol. A **16**, 1000 (1998).
[17] P. Lambin, J. P. Vigneron, and A. A. Lucas, Phys. Rev. B **32**, 8203 (1985).
[18] P. Lambin, J. P. Vigneron, and A. A. Lucas, Comput. Phys. Commun. **60**, 351 (1990).
[19] Y. T. Chu, J. B. Bates, C. W. White, and G. C. Farlow, J. Appl. Phys. **64**, 3727 (1988).
[20] J. J. Rechtien, C. R. Kannewurf, and J. O. Brittain, J. Appl. Phys. **38**, 3045 (1967).
[21] H. Ibach, H. D. Bruchmann, and H. Wagner, Appl. Phys. A: Solids Surf. **29**, 113 (1982).
[22] P. Senet, P. Lambin, J. P. Vigneron, I. Derycke, and A. A. Lucas, Surf. Sci. **226**, 307 (1990).
[23] F. S. Ohuchi and R. H. French, J. Vac. Sci. Technol. A **6**, 1695 (1987).
[24] W. J. Gignac, R. S. Williams, and S. P. Kowalczyk, Phys. Rev. B **32**, 1237 (1985).
[25] S. Ciraci and I. P. Batra, Phys. Rev. B **28**, 982 (1983).
[26] R. H. French, J. Am. Ceram. Soc. **73**, 477 (1990).
[27] F. Bartolucci, G. Schmitz, P. Gassmann, and R. Franchy, J. Appl. Phys. **10**, 6467 (1996).
[28] N. F. Mott and E. A. Davis, *Electronic Processes in Non-Crystalline Materials*, 2nd ed. (Clarendon, Oxford, 1979).
[29] N. F. Mott, Adv. Phys. **16**, 49 (1967).
[30] N. F. Mott, Philos. Mag. **17**, 1259 (1968).